Crystallographic, Electrochemical, and Pulsed EPR Study of Copper(II) Polyimidazole Complexes Relevant to the Metal Sites of Copper Proteins[||,⊥]

Christophe Place,*,[†] Jean-Luc Zimmermann,[‡] Etienne Mulliez,[†] Geneviève Guillot,[†] Claudette Bois,[§] and Jean-Claude Chottard[†]

Laboratoire de Chimie et Biochimie Pharmacologiques et Toxicologiques (CNRS URA 400), Université René Descartes, 45 rue des Saints Pères, 75270 Paris Cedex 06, France, Département de Biologie Cellulaire et Moléculaire, Section de Bioénergétique, CEA/Saclay, 91191 Gif-sur-Yvette, France, and Laboratoire de Chimie des Métaux de Transition, Université Pierre et Marie Curie, 75252 Paris Cedex 05, France

Received December 12, 1997

Copper(II) complexes of the following polyimidazole ligands have been synthesized: bis(imidazol-2-yl)methane (BIM), bis(imidazol-2-yl) ketone (BIK), 4-(imidazol-4-ylmethyl)-2-(imidazol-2-ylmethyl)imidazole (TRIM), bis-[4-(imidazol-4-ylmethyl)imidazol-2-yl]methane (TIM), and bis[4-(imidazol-4-ylmethyl)imidazol-2-yl] ketone (TIK). Their crystal structures have been determined using X-ray diffraction. $[Cu(ClO_4)_2(BIM)_2]$, **1**, belongs to the triclinic space group $P\bar{1}$ system, $a = 7.161(4)$ Å, $b = 7.986(6)$ Å, $c = 9.865(3)$ Å, $\alpha = 76.73(5)°$, $\beta = 71.18(3)°$, $\gamma = 76.44(5)°$, $Z = 1$, $T = 291$ K; $R = 0.035$, $R_w = 0.036$ for 1668 reflections; Cu−N = 1.998(3) and 2.001(2) Å, Cu−O = 2.574(4) Å, in a tetragonal geometry. $[Cu(BIK)_2](ClO_4)_2$, **2**, belongs to the monoclinic space group $C2/c$ system, $a = 9.029(3)$ Å, $b = 12.497(2)$Å, $c = 19.197(2)$ Å, $\beta = 94.59(2)°$, $Z = 4$, $T = 291$ K; $R = 0.056$, $R_w = 0.061$ for 1052 reflections; Cu−N = 1.961(7) and 1.954(7) Å, in a distorted tetrahedral geometry. [CuCl-(TRIM)(CH_3OH)]Cl, **6**, belongs to the monoclinic space group $P2_1/n$ system, $a = 14.192(5)$ Å, $b = 13.832(5)$ Å, $c = 7.913(3)$ Å, $\beta = 90.55(4)°$, $Z = 4$, $T = 291$ K; $R = 0.062$, $R_w = 0.057$ for 1377 reflections; Cu−N = 1.987(7), 2.007(7) and 2.007(6) Å, Cu−O = 2.521(7) Å, Cu−Cl = 2.298(2) Å, in a square pyramidal geometry. $[Cu(ClO_4)(TIM)](ClO_4)$, **4**, belongs to the triclinic space group $P\bar{1}$ system, $a = 9.604(4)$ Å, $b = 11.508(6)$ Å, $c = 12.003(8)$ Å, $\alpha = 58.79(4)°$, $\beta = 94.59(2)°$, $\gamma = 67.43(3)°$, $Z = 2$, $T = 291$ K; $R = 0.057$, $R_w = 0.062$ for 2084 reflections; Cu−N = 1.985(7), 1.964(7), 1.967(7), and 1.966(7) Å, Cu−O = 2.553(8) Å, in a distorted square pyramidal geometry. [CuCl(TIK)](ClO_4), **7**, belongs to the triclinic space group $P\bar{1}$ system, $a = 7.432(3)$ Å, $b = 12.573(3)$ Å, $c = 12.945(2)$ Å, $\alpha = 114.94(4)°$, $\beta = 92.46(2)°$, $\gamma = 103.49(3)°$, $Z = 2$, $T = 291$ K; $R = 0.043$, $R_w = 0.049$ for 2305 reflections; Cu−N = 1.984(5), 1.989(5), 2.012(5), and 1.979(5) Å, Cu−Cl = 2.796-(2) Å, in a distorted bipyramidal geometry. In methanol solution, the perchlorato complexes **1**, **2**, Cu(TRIM)-$(ClO_4)_2$ (**3**), **4**, and Cu(TIK)$(ClO_4)_2$ (**5**) exhibited redox potentials from −215 to +284 mV vs NHE together with a visible absorption from 604 to 728 nm. Electron spin-echo envelope modulation (ESEEM) spectroscopy data, particularly the nuclear quadrupole interaction (NQI) parameters e^2qQ and η of the remote nitrogen (N1H), were analyzed and interpreted according to the model devised by Jiang et al. (*J. Am. Chem. Soc.* **1990**, *112*, 9035) with reference to $Cu(HIm)_4(ClO_4)_2$. The results are the following: (i) C2 substitution of the imidazole ring, next to the remote nitrogen (**1**, **2**) decreases the asymmetry parameter η to ca. 0.75 compared to 1.00 for $Cu(HIm)_4$-$(ClO_4)_2$; this effect of C2 substitution on the symmetry of the electric field gradient at N1H appears similar for both the electron-donating methylene substituents (**1**) and the electron-withdrawing carbonyl group (**2**). (ii) The electron-donating or -withdrawing properties of the substituent are reflected by the variation of the e^2qQ parameter, increasing from 1.43 to 1.75 MHz (**1**) or decreasing to 1.38 MHz (**2**), and by the ν_+ transition shifting toward higher frequencies from 1.49 to 1.65 MHz (**1**, **3**, **4**) or to lower frequencies to 1.29 MHz (**2**, **5**). The use of the η and ν_+ parameters to assign the Nδ vs Nϵ coordination of histidine to the metal and to detect modified histidine in copper-binding proteins is discussed.

Introduction

Copper metalloproteins are involved in various biological functions such as electron transfer, oxygen transport, or substrate oxidation.[2−6] These functions are the consequence of the redox properties of the copper ion modulated by the protein ligands and of the selection of substrates by the active site. Modulation of the reactivity is obtained mainly by changing the coordination around the copper (number, type, and geometry).[7] This is achieved in proteins by varying the amino acid ligands and their

* To whom correspondence should be addressed.
[†] Université René Descartes.
[‡] CEA/Saclay.
[§] Université Pierre et Marie Curie.

[||] Abbreviations: HIm, imidazole; BIM, bis(imidazol-2-yl)methane; BIK, bis(imidazol-2-yl)ketone; TRIM, 4-(imidazol-4-ylmethyl)-2-(imidazol-2-ylmethyl)imidazole; TIM, bis[4-(imidazol-4-ylmethyl)imidazol-2-yl]methane; TIK, bis[4-(imidazol-4-ylmethyl)imidazol-2-yl] ketone; ESEEM, electon spin-echo envelope modulation; NQI, nuclear quadrupole interaction; NMR, nuclear magnetic resonance; SCE, saturated calomel electrode; NHE, normal hydrogen electrode.

[⊥] Formulas: In the text, the formulas of the complexes appear written either according to IUPAC nomenclature for the compounds characterized by an X-ray structure (e.g.; [CuCl(TRIM)(CH_3OH)]Cl) or according to the stoichiometric composition for the other compounds (e.g., Cu(TRIM)-$(ClO_4)_2$).

S0020-1669(97)01566-8 CCC: $15.00
Published on Web 07/23/1998

arrangement at the active site. The corresponding modifications of the electronic structure are reflected by the variation of the spectral characteristics and redox potential of the metal center.[8−11] Modeling of the metal-binding site of metalloproteins is a contribution to the understanding of their mechanism of action.[12,13] Two objectives are often pursued simultaneously, which are to reproduce both the spectral features and the reactivity of protein active sites using low molecular weight compounds susceptible to exhaustive investigation by all the physicochemical techniques available.[14,15] One of the difficulties of the model approach is to synthesize complexes with biologically relevant ligands. The imidazole of histidine is a ubiquitous ligand which is present in all types of copper active sites.[11] In very few model compounds are imidazole or polyimidazole ligands present. Commonly, aliphatic amines and imines or, more closely related to the imidazole ring, pyridine, pyrazole, and benzimidazole are used.[16−19] We have developed a general synthesis of polyimidazole ligands to model multihistidine coordination.[20] They are composed of two, three, and four imidazole rings linked by methylene or keto bridges. They are presented in Chart 1 together with the abbreviations used in the text: bis(imidazol-2-yl)methane (BIM), bis(imidazol-2-yl) ketone (BIK), 2-(imidazol-2-ylmethyl)-4-(imidazol-4-ylmethyl)imidazole (TRIM), bis[4-(imidazol-4-ylmethyl)imidazol-2-yl]methane (TIM), and bis[4-(imidazol-4-ylmethyl)imidazol-2-yl] ketone (TIK). The aim of this study was to investigate the various types of coordination of these ligands to copper and the properties of the derived complexes. They have all been characterized and their crystallographic structures resolved. The geometries of the complexes are compared and related to their redox potentials.

Among the spectroscopic methods successfully applied to study copper protein active sites, Peisach et al.[21,22] have developed ESEEM spectroscopy, which is a valuable tool to analyze the copper coordination sphere. ESEEM spectroscopy is a pulsed EPR spectroscopy which allows the measurement of small magnetic interactions between the electronic spin of Cu(II) and the nuclear spins of the neighboring nuclei.[23] Imidazole ligands were determined to belong to three groups depending on the substitution pattern of the ring.[1] We have applied ESEEM spectroscopy to our series of Cu(II) complexes, representing various types of imidazole coordination, and compared their features to those of $Cu(HIm)_4(ClO_4)_2$ used as a reference compound. The relevance of our data to those reported for Cu(II) proteins is discussed.

Chart 1. Schematic Drawings of the Polyimidazole Ligands Bis(imidazol-2-yl)Methane (BIM), Bis(imidazol-2-yl) Ketone (BIK), 2-(Imidazol-2-ylmethyl)-4-(imidazol-4-ylmethyl)imidazole (TRIM), Bis[4-(imidazol-4-ylmethyl)-imidazol-2-yl]methane (TIM), and Bis[4-(imidazol-4-yl-methyl)imidazol-2-yl] Ketone (TIK)

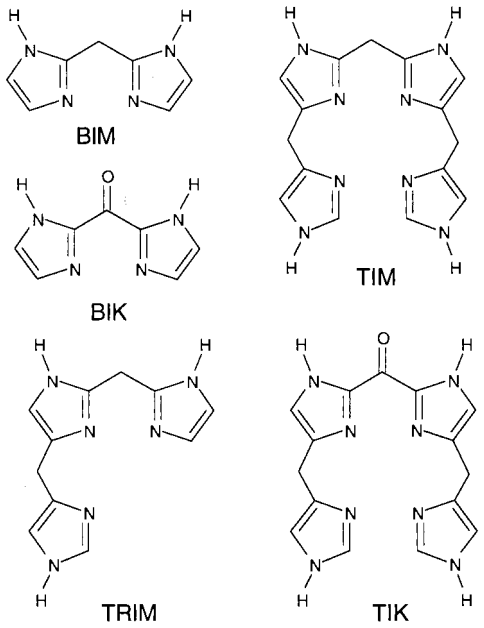

Experimental Section

Synthesis of the Ligands. The synthesis of BIM[24] and BIK[25,26] ligands has been previously described. The TRIM and TIM syntheses were reported by our group.[20] The TIK ligand was prepared via the iron-catalyzed oxidation of TIM: A 2 g sample of TIM (M_r = 344, 5.81 mmol) is dissolved in 1 L of pure methanol saturated with oxygen at room temperature. To this solution is added 50 mg of anhydrous $FeCl_3$ (M_r = 162.5, 0.31 mmol, 1:20 TIM equiv) in 5 mL of methanol after complete solubilization of the TIM. The colorless solution becomes deep blue. After 24 h of stirring, the conversion of TIM into TIK is complete (as shown by 90 MHz ^{1}H NMR monitoring). After addition of 10 mL of 4 M hydrochloric acid, the solution is evaporated and the white solid is washed with 50 mL of absolute ethanol and filtered off. The solid obtained is dissolved in pure water and slowly precipitated by addition of sodium bicarbonate, leading to 1.54 g of a white powder of $TIK{\cdot}H_2O{\cdot}{}^1/_2CH_3OH$ (M_r = 356, 4.3 mmol, 75%). Anal. Found (calcd) for $C_{15.5}H_{18}N_8$: C, 52.19 (52.24); H, 4.94 (5.05); N, 31.81 (31.46). ^{1}H NMR CD_3OD (ppm): 7.61 (s, H2, 1H), 7.09 (s, H5, 1H), 6.88 (s, H5′,1H), 3.94 (s, CH_2, 2H).

Synthesis of the Complexes. The copper salts were purchased from Alfa. Among the following complexes, **1**, **2**, and **4** have a fully characterized coordination sphere from X-ray crystallography (*vide*

(1) Jiang, F.; McCracken, J.; Peisach, J. *J. Am. Chem. Soc.* **1990**, *112*, 9035.
(2) *Copper Proteins and Copper Enzymes*; Lontie, R., Ed.; CRC Press: Boca Raton, FL, 1984; Vols. I−III.
(3) *Copper Proteins*; Spiro, T. G., Ed.; Wiley-Interscience: New York, 1981.
(4) Owen, C. A. J. *Biochemical Aspects of Copper*; Park Ridge: New York, 1982.
(5) Beinert, H. *J. Inorg. Biochem.* **1991**, *44*, 173.
(6) Fausto da Silva, J. J. R.; Williams, R. J. P. *The Biological Chemistry of the Elements*; Oxford University Press: Oxford, U.K., 1991.
(7) Solomon, E. I.; Lowery, M. D.; Root, D. E.; Hemming, B. L. *Mechanistic Bioinorganic Chemistry*; American Chemical Society: Washington, DC, 1995.
(8) Gray, H. B.; Solomon, E. I. *Copper Proteins*; Wiley-Interscience: New York, 1981.
(9) Solomon, E. I.; Lowery, M. D. *Science* **1993**, *259*, 1575.
(10) Solomon, E. I.; Lowery, M. D.; LaCroix, L. B.; Root, D. E. *Methods Enzymol.* **1993**, *226*, 1.
(11) Solomon, E. I.; Penfield, K. W.; Wilcox, D. E. *Struct. Bonding* **1983**, *53*, 1.
(12) Karlin, K. D. *Science* **1993**, *261*, 701.
(13) Sorrell, T. N. *Tetrahedron* **1989**, *45*, 63.
(14) Lippard, S. J.; Berg, J. M. *Principles of Bioinorganic Chemistry*; University Science Books: Mill Valley, CA, 1993.
(15) Solomon, E. I.; Kirk, M. L.; Gamelin, D. R.; Pulver, S. *Methods Enzymol.* **1995**, *246*, 71.
(16) Ibers, J. A.; Holm, R. H. *Science* **1980**, *209*, 223.
(17) Murphy, B. P. *Coord. Chem. Rev.* **1993**, *124*, 63.
(18) Mani, F. *Coord. Chem. Rev.* **1992**, *120*, 325.
(19) Kitajima, N. *Adv. Inorg. Chem.* **1992**, *39*, 1.
(20) Mulliez, E. *Tetrahedron Lett.* **1989**, *30*, 6169.
(21) Mims, W. B.; Peisach, J. *Biological Magnetic Resonance*; Plenum Press: New York, 1981; p 213.
(22) Mims, W. B.; Peisach, J. *Biological Applications of Magnetic Resonance*; Academic Press: New York, 1979; p 221.
(23) Mims, W. B.; Peisach, J. *J. Chem. Phys.* **1978**, *69*, 4921.
(24) Joseph, M.; Leigh, T.; Swain, M. L. *Synthesis* **1977**, 459−60.
(25) Gorun, S. M.; Papaefthymiou, G. C.; Frankel, R. B.; Lippard, S. J. *J. Am. Chem. Soc.* **1987**, *109*, 4244.
(26) Guillot, G.; Mulliez, E.; Leduc, P.; Chottard, J. C. *Inorg. Chem.* **1990**, *29*, 579.

Table 1. Experimental Data for the Crystallographic Analysis of $[Cu(ClO_4)_2((BIM)_2]$, **1**, $[Cu(BIK)_2](ClO_4)_2$, **2**, [CuCl(TRIM)(CH_3OH)]Cl, **6**, [Cu(ClO_4)(TIM)](ClO_4), **4**, and [CuCl(TIK)](ClO_4), **7**

	1	**2**	**6**	**4**	**7**
crystal system	triclinic	monoclinic	monoclinic	triclinic	triclinic
space group	$P\bar{1}$	$C2/c$	$P2_1/n$	$P\bar{1}$	$P\bar{1}$
a, Å	7.161(4)	9.029(3)	14.192(5)	9.604(4)	7.432(3)
b, Å	7.986(6)	12.497(2)	13.832(5)	11.508(6)	12.573(3)
c, Å	9.865(3)	19.197(5)	7.913(3)	12.003(8)	12.945(2)
α, deg	76.73(5)	90	90	58.79(4)	114.94(1)
β, deg	71.18(3)	94.59(2)	90.55(4)	71.82(4)	12.573(3)
γ, deg	76.44(5)	90	90	67.43(3)	103.49(2)
V, Å^3	512(1)	2159(2)	1553(2)	1037(3)	1052(2)
Z	1	4	4	2	2
d_{calc}, g cm^{-3}	1.81	1.80	1.69	1.83	1.74
μ, cm^{-1}	13.9	13.3	18.1	13.7	13.5
no. of indep reflns	1812	1882	2720	2975	3688
no. of reflns used[a]	1668	1052	1377	2084	2305
R[b]	0.035	0.056	0.062	0.057	0.043
R_w[b]	0.036	0.061	0.057	0.062	0.049

[a] With $I \geq 3\sigma(I)$. [b] $R = \sum(|F_o| - |F_c|)/\sum|F_o|$ and $R_w = [\sum w(|F_o| - |F_c|)^2/\sum w|F_o|^2]^{1/2}$.

infra) and the others, **3** and **5**, correspond to a stoichiometry which is confirmed by the X-ray structure of their monochloro derivatives **6** and **7**, respectively (vide infra).

(a) $[Cu(ClO_4)_2(BIM)_2]$, 1. A 2 mL colorless methanol solution of 105.8 mg (M_r = 148, 0.714 mmol) of BIM is added to a pale blue solution of 132.4 mg (M_r = 370.5, 0.357 mmol) of $Cu(ClO_4)_2 \cdot 6H_2O$ in 2 mL of methanol. The solution immediately turns deep purple. After 5 min of stirring, the complex spontaneously precipitates, leading to 161 mg of a deep purple powder of $[Cu(ClO_4)_2(BIM)_2]$ (M_r = 558.5, 0.288 mmol, 81%). Anal. Found (calcd) for $C_{14}H_{16}N_8O_8Cl_2Cu$, C, 30.19 (30.08); H, 2.94 (2.86); N, 19.90 (20.05); Cl, 13.08 (12.69); Cu, 11.17 (11.37).

(b) $[Cu(BIK)_2](ClO_4)_2$, 2. A 4 mL colorless methanol solution of 164.8 mg (M_r = 162, 1.01 mmol) of the BIK ligand is added to a pale blue solution of 188.5 mg (M_r = 370.5, 0.508 mmol) of $Cu(ClO_4)_2 \cdot 6H_2O$ in 2 mL of methanol. The solution immediately turns green, and after 5 min, 182 mg of small green needles of $[Cu(BIK)_2](ClO_4)_2$ (M_r = 586.5, 0.31 mmol, 61%) precipitates. Anal. Found (calcd) for $C_{14}H_{12}N_8O_{10}Cl_2Cu$: C, 28.90 (28.64); H, 2.10 (2.04); N, 18.63 (19.09); Cl, 11.92 (12.09); Cu, 10.79 (10.83).

(c) $Cu(TRIM)(ClO_4)_2$, 3. A 1 mL pale yellow methanol solution of 92.56 mg (M_r = 228, 0.406 mmol) of the TRIM ligand is added to a pale blue solution of 150.5 mg (M_r = 370.5, 0.406 mmol) of $Cu(ClO_4)_2 \cdot 6H_2O$ in 2 mL of methanol. The solution immediately turns green, and after 5 min of stirring, 148 mg of a green precipitate of $Cu(TRIM)(ClO_4)_2$ (M_r = 490.5, 0.3 mmol, 74%) is obtained. Anal. Found (calcd) for $C_{11}H_{12}N_6O_8Cl_2Cu$: C, 26.49 (26.91); H, 2.95 (2.44); N, 15.63 (17.12); Cl, 14.78 (14.45); Cu, 9.05 (12.95). The Cu and N values could not be obtained in good agreement with the calculated ones. This could reflect the presence of one molecule of methanol solvent in the coordination sphere giving the following analysis. Found (calcd) for $C_{12}H_{16}N_6O_9Cl_2Cu$: C, 26.49 (27.55); H, 2.95 (3.06); N, 15.63 (16.07); Cl, 14.78 (13.58); Cu, 9.05 (12.15). This does not fit well either. However, the crystallographic data for the chloro instead of the perchlorato complex **6** show that it indeed contains both one chloride and one methanol ligand (*vide infra*).

(d) $[Cu(ClO_4)(TIM)](ClO_4)$, 4. A 2 mL methanol colorless solution of 129.6 mg (M_r = 380, 0.377 mmol) of TIM is added to a pale blue solution of 139.6 mg (M_r = 370.5, 0.377 mmol) of $Cu(ClO_4)_2 \cdot 6H_2O$ in 2 mL of methanol. The solution becomes deep blue, and after stirring, followed by slow diffusion of ether, a precipitate of 138 mg of the blue complex $[Cu(ClO_4)(TIM)](ClO_4)$ (M_r = 570.5, 0.242 mmol, 64%) is obtained. Anal. Found (calcd) for $C_{15}H_{16}N_8O_8Cl_2Cu$: C, 32.38 (31.55); H, 3.11 (2.80); N, 19.87 (19.63); Cl, 12.44 (12.42); Cu, 9.98 (11.10).

(e) $Cu(TIK)(ClO_4)_2$, 5. A 4 mL methanol pale yellow solution of 136.35 mg (M_r = 356, 0.383 mmol) of $TIK \cdot H_2O \cdot {}^1/_2CH_3OH$ is added to a pale blue solution of 139.6 mg (M_r = 370.5, 0.377 mmol) of $Cu(ClO_4)_2 \cdot 6H_2O$ in 2 mL of methanol. The solution turns blue after stirring, and a pale blue precipitate of 140 mg of $Cu(TIK)(ClO_4)_2$ (M_r = 584.5, 0.24 mmol, 63%) is obtained after slow diffusion of ether. Anal. Found (calcd) for $C_{15}H_{14}N_8O_9Cl_2Cu$: C, 31.58 (30.79); H, 2.56 (2.39); N, 19.07 (19.16); Cl, 12.76 (12.13); Cu, 10.15 (10.87).

NB. Warning! Compounds described here contain perchlorate anions. Although no accident has occurred, the use of perchlorate is hazardous because of the possibility of explosion, especially when the compounds are anhydrous.

Crystallogenesis. Several methods have been used to obtain monocrystals of complexes suitable for X-ray diffraction. Crystals of perchlorato complexes were obtained for **1**, **2**, and **4**. Crystallization of **3** was not successful, and only the chloro complex [CuCl(TRIM)-(CH_3OH)]Cl, **6**, was crystallized. **5** was crystallized in the presence of LiCl, leading to the inner-sphere chloro and outer-sphere perchlorato complex [CuCl(TIK)](ClO_4), **7**.

For $[Cu(ClO_4)_2(BIM)_2]$, **1**, slow evaporation of a dilute methanol solution led after 2 days to square deep purple crystals. For $[Cu(BIK)_2]$-$(ClO_4)_2$, **2**, a diffusor with a No. 4 sintered disk was used, containing a methanol solution of $Cu(ClO_4)_2 \cdot 6H_2O$ (1 equiv) in one compartment and a methanol solution of BIK (2 equiv) in the other. Slow diffusion through the sintered disk led to crystallization of green square monocrystals in the copper compartment. [CuCl(TIK)](ClO_4), **7**, was also crystallized using a diffusor technique. A methanol solution of $Cu(TIK)(ClO_4)_2$, **5**, with 1 equiv of LiCl was placed in one compartment while acetonitrile, a nonsolvent, was placed in the other compartment. After 3 weeks, square blue crystals were obtained. [CuCl(TRIM)(CH_3-OH)]Cl, **6**, was formed from the stoichiometric reaction of $CuCl_2$ with TRIM in methanol, and crystals were obtained by slow diffusion of ether into the solution. [Cu(ClO_4)(TIM)](ClO_4), **4**, crystals were similarly obtained by slow diffusion of ether into a methanol solution of the complex.

Crystallography. For the five compounds, unit cell dimensions with estimated standard deviations were obtained from least-squares refinements of the setting angles of 25 well-centered reflections. Two standard reflections were monitored periodically; they showed no change during data collection, except for compound **6**, for which a correction had to be applied (the decay was 14%). Crystallographic data are summarized in Table 1, and complementary information is given as Supporting Information. Corrections were made for Lorentz and polarization effects. Empirical absorption corrections (Difabs)[27] were applied. A secondary extinction correction was unnecessary, except for compounds **1** and **6**.

Computations were performed by using the PC version of CRYSTALS.[28] Atomic form factors for neutral Cu, Cl, N, O, C, and H were taken from the literature.[29] Real and imaginary parts of anomalous

(27) Walker, N.; Stuart, D. *Acta Crystallogr.* **1983**, *A39*, 158.
(28) Watkin, D. J.; Carruthers, J. R.; Betteridge, P. W. *Crystals User Guide*; Chemical Crystallography Laboratory: Oxford, U.K., 1988.
(29) *International Tables for X-ray Crystallography*; Kynoch Press: Birmingham, U.K., 1974; Vol. IV.

dispersion were taken into account. The structures were solved by direct methods (SHELXS)[30] and successive Fourier maps. All hydrogen atoms were found on difference maps; their positions were not refined, and they were given an overall isotropic thermal parameter. Non-hydrogen atoms were anisotropically refined. Full-matrix least-squares refinements were carried out by minimizing the function $\sum w(F_o - |F_c|)^2$ where F_o and F_c are the observed and calculated structure factors, except for compound **7**, where refinements were carried out in three blocks. Models reached convergence with $R = \sum(|F_o| - |F_c|)/\sum|F_o|$ and $R_w = [\sum w(|F_o| - |F_c|)^2/\sum w|F_o|^2]^{1/2}$ having the values listed in Table 1. For compound **6**, in the last stages of the refinement, each reflection was assigned a weight $w = w'[1 - (|F_o| - |F_c|)/6\sigma|F_o|)^2]^2$ with $w' = 1/\sum_r A_r T_r(X)$ with coefficients 2.20, −0.25, and 1.67 for a Chebyshev series, for which $X = F_o/F_o(\text{max})$. For the other compounds the weighting factor was unity.

Criteria for a satisfactory complete analysis were the ratios of rms shifts to standard deviations being less than 0.1 and no significant features in the last difference map.

Representations of the complexes are CAMERON[31] views of the molecules.

Electronic Spectroscopy. UV−visible spectra were recorded on a Uvikon 820 spectrophotometer, in methanol solution, at room temperature, over the wavelength range 220−800 nm. A baseline for pure methanol in a 3 mL cuvette was subtracted from the experimental spectra over the whole range observed. A millimolar concentration of each complex was used in the visible region.

Electrochemistry. Cyclic voltammograms were obtained with an EGG-PAR model 173 potentiostat and model 276 interface. The electrode system consisted of an NaCl-saturated calomel electrode as the reference electrode, a platinum electrode as the auxiliary electrode, and a glassy carbon electrode as the working electrode. The spectra were recorded at room temperature in methanol solution with a 10 mM concentration of the complexes. The scanning rate was 50 $mV \cdot s^{-1}$. $LiClO_4$ was used as the supporting electrolyte (0.1 M).

EPR and ESEEM. EPR and ESEEM studies were performed with ca. millimolar samples of the compounds in CH_3OH/H_2O solutions (1/1, v/v). EPR spectra were recorded with a Bruker ER 300 spectrometer at a temperature of 4.2 K, a nominal microwave power of 2 mW, and a modulation amplitude of 2 G. A Bruker ER 380 pulsed EPR spectrometer equipped with a dielectric resonator that allows adjustment of the loaded Q value was employed for ESEEM measurements. The spectra were obtained at a 4.2 K by recording the stimulated echo resulting from a three-microwave-pulse sequence ($\pi/2-\tau-\pi/2-T-\pi/2$) with incrementing time T.[32] The spectra were recorded with a magnetic field setting of 3400 G (see figure captions), i.e., near $g_\perp$, where the echo amplitude is maximum. ESEEM data were also occasionally recorded at other magnetic field positions and gave similar spectra in terms of the positions of the frequency peaks from ^{14}N. Time τ was chosen as twice the Larmor period of protons to suppress the contribution from weakly coupled protons to the echo envelope.[21] Fourier transformation of the time domain data was performed after suitable reconstruction of the missing points due to deadtime.[33]

Results

Description of the Structures. (a) $[Cu(ClO_4)_2(BIM)_2]$, 1. A CAMERON view is presented in Figure 1, and selected interatomic bond lengths and angles are given in Table 2. The copper is in an N_4O_2 environment with four nitrogens from imidazoles and two oxygens from the perchlorato ligands. The nitrogens define a square planar environment around the copper while the oxygens are in apical positions. The copper is at the center of symmetry of the molecule and lies in the plane defined by the four nitrogens. The shorter bonds are those between copper and nitrogen close to 2 Å, Cu−N(1) = 1.998(3) and Cu−N(2) = 2.001(2) Å, and the longer ones are the Cu−O bonds with Cu−O = 2.668(3) Å (Table 2). This suggests a weak interaction between the copper and the perchlorato groups. The angle of chelation, N(1)CuN(3) = 87.7(1)°, is smaller than the interligand angle, N(1)CuN(3)′ = 92.3(1)°, and the angle N(1)CuO(1) is close to 90°. However, despite these small distortions the six atoms around the copper define a tetragonal symmetry. The copper environment is very similar to that found for $[Cu(SO_4)_2(HIm)_4]$.[34]

(b) $[Cu(BIK)_2](ClO_4)_2$, 2. A CAMERON view is presented in Figure 1, and selected interatomic bond lengths and angles are given in Table 2. The copper is tetracoordinated in an N_4 environment. There is no interaction between the copper and the perchlorato counterions. The four nitrogens belong to the two BIK chelates. The distances between the copper and the nitrogens are short, with Cu−N(1) = 1.961(7) and Cu−N(3) = 1.954(7) Å, compared to those found for $[Cu(ClO_4)_2(BIM)_2]$ and $[Cu(SO_4)_2(HIm)_4]$. This indicates a strong coordination of the imidazoles to the copper. A strong deviation from planar geometry is observed: the angles N(1)CuN(1)′ and N(3)CuN(3)′ are 140.2(4) and 147.5(4)°, respectively, instead of 180° for planar geometry, and the angle between the planes N(1)CuN(3) and N(1)′CuN(3)′ is equal to 125.6° instead of 180°. We conclude that **2** is best seen as a distorted tetrahedral structure. The strong difference between **2** and **1** is due to the rigidity imposed by the keto group which does not allow a sufficient torsion of the bis(imidazolyl)methane moiety necessary to avoid the repulsion between the C(7) (C(7)′) and C(1)′ (C(1)) hydrogens which would occur if the two BIK ligands were coplanar.

(c) $[CuCl(TRIM)(CH_3OH)]Cl$, 6. A CAMERON view is presented in Figure 1, and selected interatomic bond lengths and angles are given in Table 2. The first coordination shell is composed of five atoms: N_3OCl. The three nitrogens belong to the imidazoles, the oxygen comes from a molecule of methanol, and the chloride is a bound counterion. The strength of the Cu−N bonds is of the same order as those found in **1**, with Cu−N distances close to 2 Å. The Cu−O bond length is shorter than that with the perchlorato ligand, 2.326(7) Å, and the Cu−Cl bond is short, at 2.298(2) Å. The bound nitrogens and the chloride form a plane while the oxygen is in an axial position. The copper lies only 0.023 Å above this plane. Close observation of the structure shows the presence of the chloride counterion in the other apical position but at a long distance from the copper (3.259(3) Å). Thus the copper environment in **6** is a distorted tetragonal arrangement close to a square pyramid.

(d) $[Cu(ClO_4)(TIM)](ClO_4)$, 4. A CAMERON view is presented in Figure 1, and selected interatomic bond lengths and angles are given in Table 2. The copper is surrounded by five ligands forming an N_4O environment. The four nitrogens belong to the four imidazoles of TIM, and the oxygen is from bound perchlorato counterion. The Cu−N distances are short, with Cu−N(1) close to 1.985(7) Å and Cu−N(3), Cu−N(5), and Cu−N(7) close to 1.965 Å. All the Cu−N distances are smaller than 2 Å, indicating a strong coordination of the imidazoles. The oxygen with a Cu−O distance of 2.553(8) Å is coordinated to the copper with a bond length comparable to that of the methanol−copper bond in $[CuCl(TRIM)(CH_3OH)]Cl$ or of the sulfato−copper bond in $[Cu(SO_4)_2(HIm)_4]$. The

(30) Sheldrick, G. M. *SHELXS: Program for Crystal Structure Solution;* University of Göttingen: Göttingen, Germany, 1986.
(31) Pearce, L. J.; Watkin, D. J. *CAMERON*; Chemical Crystallography Laboratory: Oxford, U.K., 1992.
(32) Kevan, L. *Modern Pulsed and Continuous Wave Electron Spin Resonance*; Wiley-Interscience: New York, 1990; p 231.
(33) Mims, W. B. *J. Magn. Reson.* **1984**, *59*, 291.
(34) Lundberg, B. K. S. *Acta Chem. Scand.* **1972**, *26*, 3977.

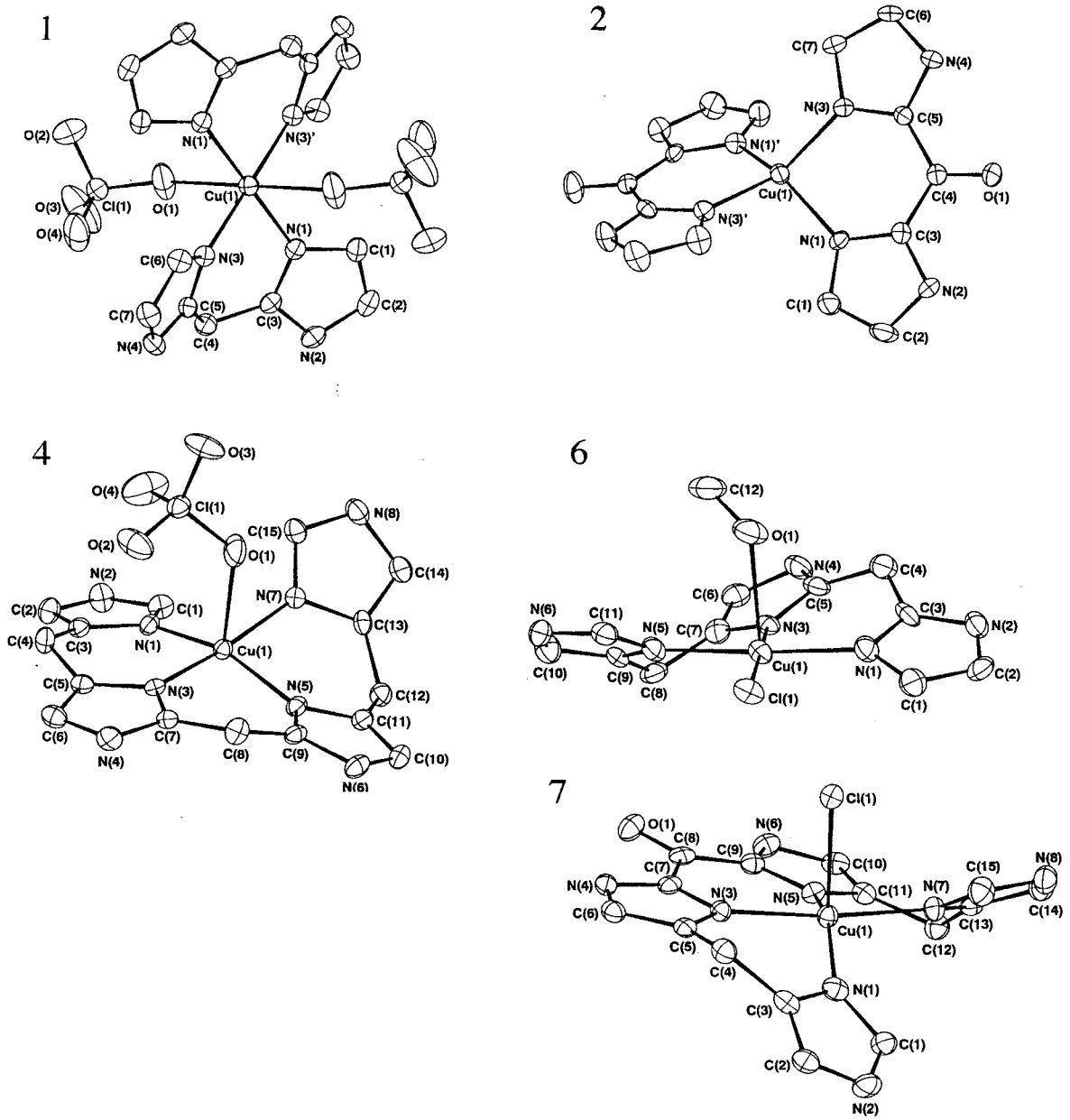

Figure 1. CAMERON representations of $[Cu(ClO_4)_2(BIM)_2]$, **1**, $[Cu(BIK)_2](ClO_4)_2$, **2**, $[Cu(ClO_4)(TIM)](ClO_4)$, **4**, $[CuCl(TRIM)(CH_3OH)]Cl$, **6**, and $[CuCl(TIK)](ClO_4)$, **7**, with the atomic labeling. For clarity, the hydrogens are omitted.

main angles show a strong distortion from tetragonal symmetry with N(1)CuN(5) = 156.0(3)° and N(3)CuN(7) = 168.6(3)°. The four nitrogens strongly deviate from the plane of a tetragonal geometry of which the perchlorato oxygen occupies an apical position. Since no interaction appears in the trans apical position and since the copper lies above the mean plane of the nitrogens in the direction of the single perchlorato ligand, the geometry of **4** can be seen as that of a distorted square planar pyramid.

(e) [CuCl(TIK)](ClO$_4$), 7. A CAMERON view is presented in Figure 1, and selected interatomic bond lengths and angles are given in Table 2. The copper is coordinated by five ligands which form an N_4Cl environment.These are the four imidazoles of TIK and one chloride counterion. The Cu−N distances are slightly smaller than 2 Å and close to the values found for $[Cu(SO_4)_2(HIm)_4]$. The chloride is not strongly coordinated, with a bond length of 2.796(2) Å, longer than that observed for the chloride ligand in $[CuCl(TRIM)(CH_3OH)]Cl$. The coordination sphere in **7** shows a strong distortion from tetragonal to trigonal bipyramidal geometry with N(1)N(5)Cl in a plane and N(3),N(7) in axial positions. Accordingly, the angles N(1)CuN(5), N(5)CuCl, and N(1)CuCl exhibit respective values of 149.7(2), 114.5(1), and 95.6(2)°, which are intermediate between the corresponding tetragonal and bipyramidal values, i.e., 180−120° for the first and 90−120° for the other two.

Visible Spectroscopy. All the complexes present an absorption in the visible region. These absorptions are weak with a large Gaussian shape centered at 600−630 nm, except that for the $Cu(BIK)_2^{2+}$ chromophore, whose maximum appears at a 100 nm longer wavelength, 728 nm (Table 3). The beginning of a band in the near-infrared region is also observed. The former bands are attributed to the forbidden d−d transitions between the electronic states of the copper.[11,35] Three transitions are expected between the $^2B_2$ ground state and the $^2B_1$, $^2A_1$, and $^2E_1$ excited states of tetragonal symmetry. The energy of

(35) Solomon, E. I.; Baldwin, M. J.; Lowery, M. D. *Chem. Rev.* **1992**, *92*, 521.

Table 2. Selected Interatomic Bond Lengths (Å) and Angles (deg) for $[Cu(ClO_4)_2((bim)_2]$, **1**, $[Cu(BIK)_2](ClO_4)_2$, **2**, $[CuCl(TRIM)(CH_3OH)]Cl$, **6**, $[Cu(ClO_4)(TIM)](ClO_4)$, **4**, and $[CuCl(TIK)](ClO_4)$, **7**

	$[Cu(ClO_4)_2(BIM)_2]$, **1**		
Cu(1)N(1)	1.998(3)	Cu(1)N(3)	2.000(2)
Cu(1)O(1)	2.689(3)		
N(1)Cu(1)N(1′)	180	N(1)Cu(1)N(3)	87.7(1)
N(1)Cu(1)N(3′)	92.3(1)	N(3)Cu(1)N(3′)	180
N(1)Cu(1)O(1)	87.8(1)	N(1)Cu(1)O(1′)	92.2(1)
N(3)Cu(1)O(1)	92.39(9)	N(3)Cu(1)O(1′)	87.61(9)
O(1)Cu(1)O(1′)	180		
	$[Cu(BIK)_2](ClO_4)_2$, **2**		
Cu(1)N(1)	1.961(7)	Cu(1)N(3)	1.954(7)
N(1)Cu(1)N(1′)	140.2(4)	N(1)Cu(1)N(3)	93.7(3)
N(3)Cu(1)N(1′)	97.2(3)	N(3)Cu(1)N(3′)	147.5(4)
	$[CuCl(TRIM)(CH_3OH)]Cl$, **6**		
Cu(1)N(1)	1.955(7)	Cu(1)N(3)	2.008(6)
Cu(1)N(5)	2.980(7)	Cu(1)Cl(1)	2.298(2)
Cu(1)O(1)	2.326(7)	Cu(1)Cl(2)	3.259(3)
N(1)Cu(1)Cl(1)	93.0(2)	N(3)Cu(1)Cl(1)	175.6(2)
N(1)Cu(1)N(3)	88.7(3)	N(5)Cu(1)Cl(1)	90.9(2)
N(1)Cu(1)N(5)	175.7(3)	N(3)Cu(1)N(5)	87.6(3)
O(1)Cu(1)Cl(1)	93.7(2)	N(1)Cu(1)O(1)	92.2(3)
N(3)Cu(1)O(1)	90.4(2)	N(5)Cu(1)O(1)	85.8(3)
Cl(1)Cu(1)Cl(2)	86.98(7)	N(1)Cu(1)Cl(2)	98.1(2)
N(3)Cu(1)Cl(2)	88.4(2)	N(5)Cu(1)Cl(2)	84.1(2)
	$[Cu(ClO_4)(TIM)](ClO_4)$, **4**		
Cu(1)N(1)	1.985(7)	Cu(1)N(3)	1.964(7)
Cu(1)N(5)	1.967(7)	Cu(1)N(7)	1.966(7)
Cu(1)O(1)	2.553(8)		
N(1)Cu(1)N(3)	91.9(3)	N(1)Cu(1)N(5)	156.0(3)
N(3)Cu(1)N(5)	90.3(3)	N(1)Cu(1)N(7)	93.4(3)
N(3)Cu(1)N(7)	168.6(3)	N(5)Cu(1)N(7)	88.9(3)
N(1)Cu(1)O(1)	108.7(3)	N(3)Cu(1)O(1)	85.7(3)
N(7)Cu(1)O(1)	95.3(3)	N(5)Cu(1)O(1)	83.0(3)
	$[CuCl(TIK)](ClO_4)$, **7**		
Cu(1)N(3)	1.989(5)	Cu(1)N(5)	2.012(5)
Cu(1)N(7)	1.979(5)	Cu(1)N(1)	1.984(5)
Cu(1)Cl(1)	2.796(2)		
N(1)Cu(1)Cl(1)	95.6(2)	N(3)Cu(1)Cl(1)	84.4(1)
N(3)Cu(1)N(1)	89.4(2)	N(5)Cu(1)Cl(1)	114.5(1)
N(1)Cu(1)N(5)	149.7(2)	N(3)Cu(1)N(5)	90.5(2)
N(7)Cu(1)Cl(1)	89.3(2)	N(1)Cu(1)N(7)	94.1(2)
N(3)Cu(1)N(7)	173.0(2)	N(5)Cu(1)N(7)	89.5(2)

Table 3. Visible Spectroscopy Data for Perchlorato Copper(II) Polyimidazole Complexes in Methanol Solution at 20 °C

complex	λ_{max}, nm	molar extinction coeff, $L \cdot mol^{-1} \cdot cm^{-1}$	half-height width, nm
$[Cu(BIK)_2](ClO_4)_2$, **2**	728	86	288
$Cu(TIK)(ClO_4)_2$, **5**	636	71	256
$Cu(TRIM)(ClO_4)_2$, **3**	632	41	200
$[Cu(ClO_4)(TIM)](ClO_4)$, **4**	626	67	236
$[Cu(ClO_4)_2(BIM)_2]$, **1**	604	42	300

the band depends on the type of symmetry around the copper. For tetrahedral distortion, which is the case only for the $Cu(BIK)_2^{2+}$ chromophore, the energy difference between the various states becomes smaller as the order of the states changes[36] and then the absorption maximum is shifted to higher wavelength.

Electrochemistry. Redox semipotentials were measured by cyclic voltammetry in methanol for the copper (II) perchlorato complexes (Figure 2). All the complexes studied present a quasi-reversible process except $Cu(TIK)(ClO_4)_2$, **5** (Figure 2 (**5**)),

(36) Solomon, E. I.; Hare, J. W.; Dooley, D. M.; Dawson, J. H.; Stevens, P. J.; Gray, H. B. *J. Am. Chem. Soc.* **1980**, *102*, 168.

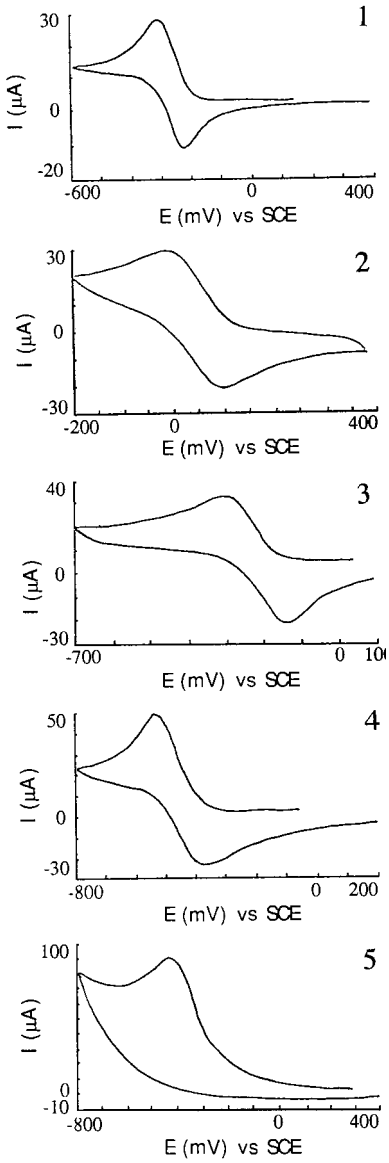

Figure 2. From top to bottom, cyclic voltammetry of $[Cu(ClO_4)_2(BIM)_2]$, **1**, $[Cu(BIK)_2](ClO_4)_2$, **2**, $Cu(TRIM)(ClO_4)_2$, **3**, $[Cu(ClO_4)(TIM)](ClO_4)$, **4**, and $Cu(TIK)(ClO_4)_2$, **5**, recorded at a glassy C electrode in deaerated methanol solution. The temperature is 20 °C. The scan rate is 0.05 V. s^{-1}. Potentials are referred to the saturated calomel electrode (SCE). To obtain a value vs the normal hydrogen electrode, 0.241 V has to be added to the SCE values.

Table 4. Cathodic (E_c) and Anodic (E_a) Potentials and $E_{1/2}$ Values for Copper(II) Polyimidazole Complexes in Methanol Solution

complex	E_c, mV vs NHE	$E_{1/2}$, mV vs NHE	E_a, mV vs NHE
$[Cu(BIK)_2](ClO_4)_2$, **2**	224	284.5	345
$Cu(TRIM)(ClO_4)_2$, **3**	−60	31	122
$[Cu(ClO_4)_2(BIM)_2]$, **1**	−60	−21.5	17
$[Cu(ClO_4)(TIM)](ClO_4)$, **4**	−291	−215.5	−140
$Cu(TIK)(ClO_4)_2$, **5**	−260		

which is not stable in the copper(I) state. The data are collected in Table 4. The $E_{1/2}$ values span a very large region from −200 to +300 mV vs NHE. The decreasing strengths of the oxidants follow the series $[Cu(BIK)_2](ClO_4)_2$, **2**, ≫ $Cu(TRIM)(ClO_4)_2$, **3**, > $[Cu(ClO_4)_2(BIM)_2]$, **1**, ≫ $[Cu(ClO_4)(TIM)](ClO_4)$, **4**, ≈ $Cu(TIK)(ClO_4)_2$, **5**.

EPR and ESEEM Studies. The EPR spectra of $Cu(HIm)_4(ClO_4)_2$ and complexes **1**−**5** were recorded at 4.2 K, and the

Table 5. NQI Frequencies Obtained from the Fourier Transformation of the ESEEM Signals, NQI Parameters of the Remote Nitrogen in Cu(II) Complexes, and the EPR Parameters $g_{||}$ and $A_{||}$ Obtained from the CW EPR Spectra

complex	ν_0, MHz	ν_-, MHz	ν_+, MHz	broad line, MHz	η^a	e^2qQ,[a] MHz	$A_{||}$, 10^{-4} cm^{-1}	$g_{||}$
$Cu(HIm)_4(ClO_4)_2$	0.77[b]	0.77[b]	1.49	4.35	1	1.51	193	2.26
$[Cu(ClO_4)_2(BIM)_2]$, **1**	0.64	1.00	1.62	4.58	0.73	1.75	180	2.202
$[Cu(BIK)_2](ClO_4)_2$, **2**	0.54	0.77	1.30	4.22	0.78	1.38	183	2.255
$Cu(TRIM)(ClO_4)_2$, **3**	0.67[b]	0.94[b]	1.64[b]	4.52			180	2.27
			1.50[c]					
$[Cu(ClO_4)(TIM)](ClO_4)$, **4**	0.70[b]	0.90[b]	1.65	4.42			190	2.22
			1.49					
$Cu(TIK)(ClO_4)_2$, **5**	0.70[b]	0.70[b]	1.28	4.22			193	2.22
			1.48					

[a] The nuclear quadrupole coupling e^2qQ and the asymmetry parameter η were estimated from the following equations: $e^2qQ = 2(\nu_+ + \nu_-)/3$; $\eta = 3\nu_0/(\nu_+ + \nu_-)$. [b] Broad line. [c] Shoulder.

Hamiltonian parameters are listed in Table 5. The $g_{||}$ parameters are spread over a narrow region from 2.20 to 2.27, and the $A_{||}$ parameters are very close, being situated between 180×10^{-4} and 193×10^{-4} cm^{-1}. They all appear in the region related to a type 2 Cu(II) biological center.

ESEEM spectroscopy can reveal magnetic interactions between the electronic spin of a paramagnetic ion and nearby nuclear spins such as those of coordinated atoms.[32] For Cu(II) compounds with imidazole type ligands, ESEEM spectra are magnetic fingerprints of the remote nitrogen atom of the imidazole ligand, which is not bound to the Cu(II). For the $m_s = +1/2$ manifold, the nuclear Zeeman and hyperfine interactions of the ^{14}N nucleus cancel each other, and the three nuclear levels are split by the nuclear quadrupole interaction (NQI).[23] This situation is known as the exact cancellation limit[37] and is characterized by a typical ESEEM spectrum with three sharp lines ν_0, ν_-, and ν_+ that are a direct measure of the NQI frequencies. In this configuration, the quadrupole coupling constant e^2qQ and the asymmetry parameter η of the electric field gradient around the ^{14}N atom can be determined from the spectra. These magnetic parameters are affected in particular by the presence of substituents on the ring, their electronic properties, and the polarization of the N−H bond.[1,38−40] Figure 3A shows the ESEEM spectrum recorded for the reference compound $Cu(HIm)_4(ClO_4)_2$ in CH_3OH/H_2O. It is very similar to the previously reported spectrum with the NQI peaks $\nu_0 \approx \nu_- \approx 0.77$ MHz and $\nu_+ = 1.49$ MHz, yielding $e^2qQ = 1.51$ MHz and $\eta = 1.00$. This latter value is only approximate because the ν_0 and ν_- frequencies are not resolved in the ESEEM spectrum. The ESEEM spectrum of $[Cu(ClO_4)_2(BIM)_2]$, **1**, is shown in Figure 3 (**1**), with the three low-frequency components $\nu_0 = 0.64$ MHz, $\nu_- = 1.00$ MHz, and $\nu_+ = 1.62$ MHz, yielding a larger quadrupole coupling constant $e^2qQ = 1.75$ MHz and an asymmetry parameter $\eta = 0.73$, characteristic of an electric field gradient of higher symmetry than that of the reference compound $Cu(HIm)_4(ClO_4)_2$. For $[Cu(BIK)_2](ClO_4)_2$, **2** (Figure 3 (**2**)), the NQI parameters are different from those of the two previous coumpounds with $e^2qQ = 1.38$ MHz and $\eta = 0.78$, and it is noteworthy that e^2qQ is now smaller than that for the reference compound. This reflects differences in the electronic properties of the remote nitrogens of the imidazole ligands in the two complexes. The ESEEM spectra of the other complexes of this study $Cu(TRIM)(ClO_4)_2$, **3**, $[Cu(ClO_4)(TIM)](ClO_4)$, **4**, and $Cu(TIK)(ClO_4)_2$, **5**, are shown in Figure 3 (**3**−**5**), respectively. The spectra are characterized by an increasing complexity due to superimposition of sets of NQI frequencies. These sets of NQI frequencies are reflected by the sole ν_+ frequency since the corresponding ν_0 and ν_- transitions are not well resolved. In fact, for $[Cu(ClO_4)(TIM)](ClO_4)$, **4**, the ν_+ peak is split into two components at 1.49 and 1.65 MHz that are assigned to the ν_+ frequencies of ^{14}N atoms with different e^2qQ parameters for the TIM ligand. A similar effect is observed in the ESEEM spectrum of $Cu(TIK)(ClO_4)_2$, **5**, with two frequencies at 1.28 and 1.48 MHz that are attributed to the ν_+ transitions of two types of ^{14}N. The ESEEM spectrum of $Cu(TRIM)(ClO_4)_2$, **3**, is less resolved in the ν_+ region. The main peak is centered at 1.64 MHz, while a shoulder, more visible at 3100 G (data not shown), is present at 1.50 MHz.

The ESEEM spectra presented in Figure 3 also show a number of lines at frequencies higher than the pure NQI frequencies. The rather broad line that appears at 4−5 MHz in all the spectra is assigned to the double-quantum transition in the ^{14}N nuclear manifold for which the hyperfine and quadrupole coupling terms add.[22] As expected, this double-quantum frequency line was observed to shift with the external magnetic field when the ESEEM was recorded at different magnetic field positions through the broad EPR line (not shown). The lines at frequencies between 2 and 3 MHz in the spectra are combination lines of the sharp NQI lines. They appear at frequencies that correspond to the sums of the NQI frequencies when the coupling involves more than one equivalent ^{14}N.[58] The ESEEM spectrum of **A**, where the central Cu(II) is bound

(37) Flanagan, H. L.; Singel, D. J. *J. Chem. Phys.* **1987**, *87*, 5606.
(38) Jiang, F.; Peisach, J. *Inorg. Chem.* **1994**, *33*, 1348.
(39) Jiang, F.; Karlin, K. D.; Peisach, J. *Inorg. Chem.* **1993**, *32*, 2576.
(40) Tran, K. C.; Battioni, J. P.; Zimmermann, J. L.; Bois, C.; Koolhaas, G. J. A. A.; Leduc, P.; Mulliez, E.; Boumchita, H.; Reedijk, J.; Chottard, J. C. *Inorg. Chem.* **1994**, *33*, 2808.
(41) Nar, H.; Messerschmidt, A.; Huber, R.; de Kamp, M. V.; Canters, G. W. *J. Mol. Biol.* **1991**, *221*, 765.
(42) Norris, G. E.; Anderson, B. F.; Baker, B. F. *J. Am. Chem. Soc.* **1986**, *108*, 2784.
(43) Baker, E. N. *J. Mol. Biol.* **1988**, *203*, 1071.
(44) Adman, E. J.; Turley, S.; Bramson, R.; Petratos, K.; Banner, D.; Tsernoglov, D.; Beppu, T.; Watanabe, H. *J. Biol. Chem.* **1989**, *264*, 87.
(45) Guss, J. M.; Harrowell, P. R.; Murata, M.; Norris, V. A.; Freeman, H. C. *J. Mol. Biol.* **1986**, *192*, 361.
(46) Redinbo, M. R.; Cascio, D.; Choukair, M. K.; Rice, D.; Merchant, S.; Yeates, T. O. *Biochemistry* **1993**, *32*, 10560.
(47) Petrakos, K.; Dauter, D.; Wilson, K. S. *Acta Crystallogr.* **1988**, *B44*, 628.
(48) Messerschmidt, A.; Rossi, A.; Ladenstein, R.; Huber, R.; Bolognesi, M.; Gatti, G.; Marchesini, A.; Petruzzelli, R.; Finazzi-Agro, A. *J. Mol. Biol.* **1989**, *206*, 513.
(49) Iitaka, Y.; Nakamura, H.; Nakatani, T.; Muraoka, Y.; Fujii, A.; Takita, T.; Umezawa, H. *Jpn. J. Antibiot.* **1978**, *31*, 1070.
(50) Avigliano, L.; Davis, J. L.; Graziani, M. T.; Marchesini, A.; Mims, W. B.; Mondovi, B.; Peisach, J. *FEBS Lett.* **1981**, *136*, 80.
(51) Mims, W. B.; Peisach, J. *J. Biol. Chem.* **1979**, *254*, 4321.
(52) Burger, R. M.; Adler, A. D.; Horwitz, S. B.; Mims, W. B.; Peisach, J. *Biochemistry* **1981**, *20*, 1701.
(53) Ito, N.; Phillips, S. E. V.; Stevens, C.; Ogel, Z. B.; McPherson, J.; Keen, J. N.; Yadav, K. D. S.; Knowles, P. F. *Nature* **1991**, *350*, 87.
(54) Kosman, D. J.; Peisach, J.; Mims, W. B. *Biochemistry* **1980**, *19*, 1304.

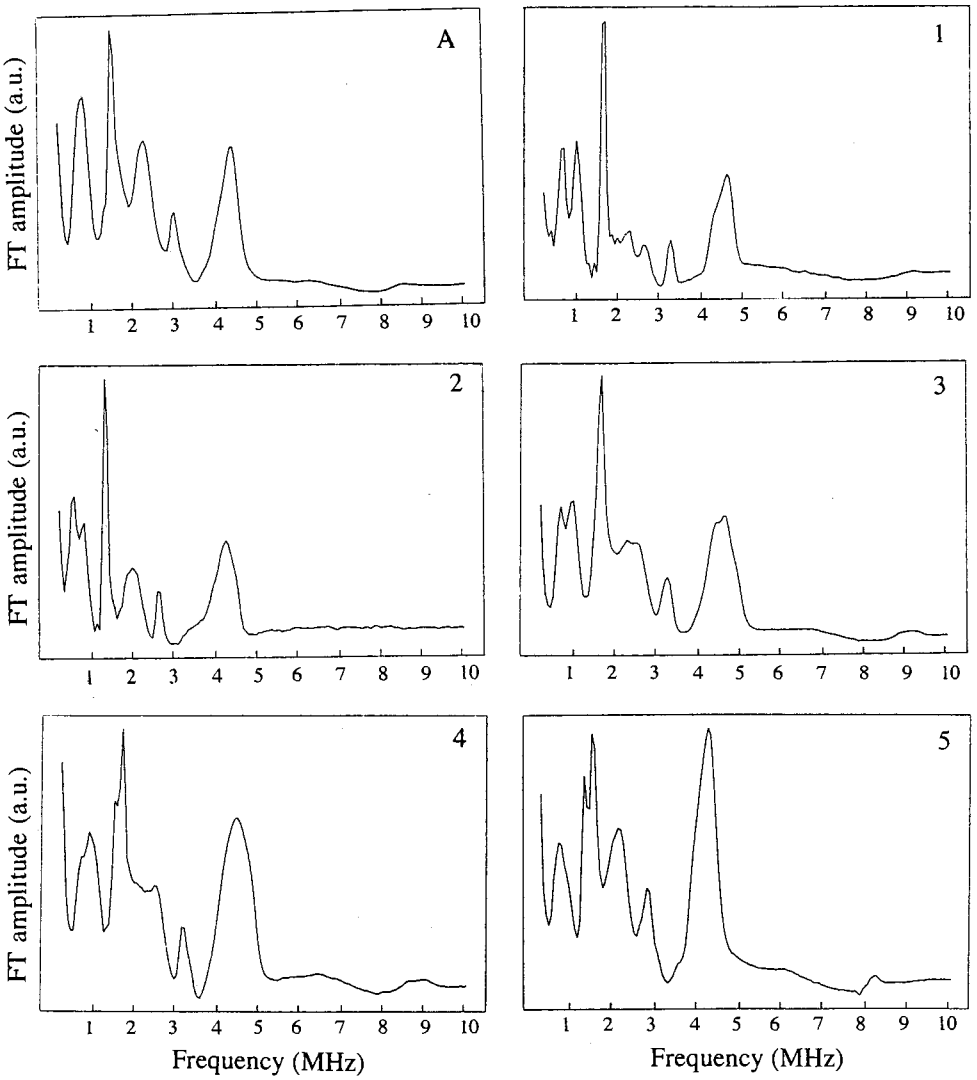

Figure 3. Three pulse Fourier transformed ESEEM spectra of $Cu(HIm)_4(ClO_4)_2$, **A**, $[Cu(ClO_4)_2(BIM)_2]$, **1**, $[Cu(BIK)_2](ClO_4)_2$, **2**, $Cu(TRIM)(ClO_4)_2$, **3**, $[Cu(ClO_4)(TIM)](ClO_4)$, **4** and $Cu(TIK)(ClO_4)_2$, **5**. The data sets were recorded at a temperature of 4.2 K, a magnetic field of $H = 3400$ G, a microwave frequency of 9.6 GHz, and a τ value of 136 ns. The interpulse time T was incremented from 88 to 6472 ns in 8-ns steps. Repetition time between successive pulse shots was 2.0 ms. The solvent was CH_3OH/H_2O (1/1). The spectra are presented with the same arbitrary units for the FT amplitude.

to four equivalent imidazoles illustrates this effect (Figure 3A): the intensity of the lines at 2.23 MHz ($\approx\nu_0 + \nu_+$) and 2.98 MHz ($\approx\nu_+ + \nu_+$) is associated with this 4-fold multiplicity. The presence of such combination lines in the ESEEM spectra of complexes **1**−**5** (Figure 3, panels (**1**−**5**)) reflects the multiplicity of the bound imidazoles in the corresponding complexes.

Discussion

The aim of this study was to correlate several characteristic properties of polyimidazole copper(II) complexes to their geometries, to the number and substitution of the imidazole ligands, and to the electronic effects of the latter. Seven complexes were synthesized and characterized. For five of them we determined the X-ray diffraction structure: $[Cu(ClO_4)_2(BIM)_2]$, **1**, $[Cu(BIK)_2](ClO_4)_2$, **2**, $[Cu(ClO_4)(TIM)](ClO_4)$, **4**, $[CuCl(TRIM)(CH_3OH)]Cl$, **6**, and $[CuCl(TIK)](ClO_4)$, **7**. The remaining two, $Cu(TRIM)(ClO_4)_2$, **3**, and $Cu(TIK)(ClO_4)_2$, **5**, which did not give satisfactory X-ray data, are related to **6** and **7**, respectively. The whole set of complexes has been used for our comparative spectroscopic studies. The complexes exhibit several types of coordination spheres: N_4O_2 for **1**, N_4 for **2**, N_4O for **4**, N_3OCl for **6**, and N_4Cl for **7**. Only $[Cu(ClO_4)_2(BIM)_2]$, **1**, presents the same coordination sphere as that of the previously described complex $[Cu(SO_4)_2(HIm)_4]$.[34] Apart from the three- or four-imidazole coordination, the remaining binding sites are occupied by perchlorato or chloride counterions or by a molecule of methanol solvent. The structures of the complexes are very different. $[Cu(ClO_4)_2(BIM)_2]$, **1**, has the usual tetragonal symmetry for copper(II), while $[Cu(ClO_4)(TIM)](ClO_4)$, **4**, and $[CuCl(TRIM)(CH_3OH)]Cl$, **6**, are distorted square pyramids, $[CuCl(TIK)](ClO_4)$, **7**, is best seen as a trigonal bipyramid, and $[Cu(BIK)_2](ClO_4)_2$, **2**, is a distorted tetrahedron. These geometries reflect a compromise between the preferred tetragonal structure for copper(II) and the steric constraints imposed by the polydentate ligands, related to the flexibility or the rigidity of the sp^3 or sp^2 carbon link between the imidazole

(55) McCracken, J.; Peisach, J.; Dooley, D. M. *J. Am. Chem. Soc.* **1987**, *109*, 4064.
(56) Fee, J. A.; Peisach, J.; Mims, W. B. *J. Biol. Chem.* **1981**, *256*, 1910.
(57) Lerch, K. *J. Biol. Chem.* **1982**, *257*, 6414.
(58) McCracken, J.; Pember, S.; Benkovic, S. J.; Villafranca, J. J.; Miller, R. J.; Peisach, J. *J. Am. Chem. Soc.* **1988**, *110*, 1069.

rings. Whereas the BIM ligand can accommodate a planar arrangement of the four binding nitrogens around the copper (Figure 1(**1**)), the planar BIK ligand cannot because it cannot avoid the two C(1)H/C(7)′H type repulsions. This leads to a pronounced tetrahedral distortion of the coordination sphere (Figure 1 (**2**)). Actually only the coordination of two independent BIM ligands allows a tetragonal structure. As soon as three or four imidazole rings are linked together, the polydentate constraints impose pentacoordination with one anionic counterion as a ligand. Such distortions are known to influence the redox potential of the metal center as reported for a series of copper complexes with substituted salen ligands.[14]

In our case, the potential values span a −215 to +285 mV region. If one assumes that the geometries observed for the solid complexes are essentially conserved in methanol solution, where the solvent could at most replace the weak anionic ligand, one can discuss the influence of the polyimidazole ligands. [Cu(BIK)$_2$](ClO$_4$)$_2$, **2**, with a tetrahedral geometry favoring copper(I), has the higher redox potential (Table 4). The likely additional influence of the electron-withdrawing keto group does not seem to play a significant role, since Cu(TIK)(ClO$_4$)$_2$, **5**, has a redox potential similar to that of [Cu(ClO$_4$)(TIM)](ClO$_4$), **4**. The perfect tetragonal symmetry of [Cu(ClO$_4$)$_2$(BIM)$_2$], **1**, stabilizes the copper(II) form, thus lowering the redox potential by 300 mV when compared to that of [Cu(BIK)$_2$](ClO$_4$)$_2$, **2**. However, with two independent BIM ligands, it can also accommodate the tetrahedral coordination of copper(I). The tetradentate coordination, distorted from planarity, which is present in [Cu(ClO$_4$)(TIM)](ClO$_4$), **4**, and Cu(TIK)(ClO$_4$)$_2$, **5** (to be compared to [CuCl(TIK)](ClO$_4$), **7**), strictly precludes the adoption of a tetrahedral structure and therefore disfavors the copper(I) form and lowers the redox potential of the complexes. In contrast, the geometry of Cu(TRIM)(ClO$_4$)$_2$, **3** (to be compared to [CuCl(TRIM)(CH$_3$OH)]Cl, **6**), is much less constrained, due to the tridentate TRIM ligand, which allows several coordination positions to be occupied by a molecule of solvent or a counterion. Because of this larger flexibility of the coordination sphere, the copper(I) is stabilized comparably to the way it is in complex **1** containing two BIM ligands ($E_{1/2}$ = 31 and −21.5 mV, respectively, ≫−215.5 mV).

The ESEEM study of our complexes was particularly attractive since variations of the substitution pattern on the imidazole rings are known to influence the position of the NQI lines. The NQI parameters e^2qQ = 1.51 MHz and η = 1.00 that were measured under our conditions for Cu(HIm)$_4$(ClO$_4$)$_2$ chosen as a reference are close to those previously reported.[1] For [Cu(ClO$_4$)$_2$(BIM)$_2$], **1**, and [Cu(BIK)$_2$](ClO$_4$)$_2$, **2**, characterized here, the asymmetry parameters $\eta \approx 0.73$ and $\eta \approx 0.78$ have smaller values than that of Cu(HIm)$_4$(ClO$_4$)$_2$ which correspond to less asymmetric electric field gradient tensors around the remote nitrogens (N−H) of the two ligands (Table 5). The values are close to those of Cu(II) complexes with imidazole ligands having an alkyl substituent at a position next to the remote nitrogen.[1] For the quadrupole coupling constants, the value measured for [Cu(ClO$_4$)$_2$(BIM)$_2$], **1**, e^2qQ = 1.75 MHz is significantly higher than that for Cu(HIm)$_4$(ClO$_4$)$_2$, whereas for [Cu(BIK)$_2$](ClO$_4$)$_2$, **2**, e^2qQ decreases to 1.38 MHz. The ν_+ frequency is also indicative of the type of substituent close to the remote nitrogen on the imidazole ring since each complex has its own signature: 1.49 for Cu(HIm)$_4$(ClO$_4$)$_2$, 1.62 for [Cu(ClO$_4$)$_2$(BIM)$_2$], **1**, and 1.30 for [Cu(BIK)$_2$](ClO$_4$)$_2$, **2**. The ESEEM properties of the other three complexes [Cu(ClO$_4$)(TIM)](ClO$_4$), **4**, Cu(TIK)(ClO$_4$)$_2$, **5**, and Cu(TRIM)(ClO$_4$)$_2$, **3**, indicate that the properties of the imidazole groups in the various ligands can be divided into three groups: the first group with NQI parameters close to those of [Cu(ClO$_4$)$_2$(BIM)$_2$], **1**, the second group with NQI parameters close to those of [Cu(BIK)$_2$](ClO$_4$)$_2$, **2**, and the third with NQI parameters close to those of Cu(HIm)$_4$(ClO$_4$)$_2$ (Table 5).

Chart 2. Conventional Numbering of the Imidazole Ring and Schematic Representation of Nδ and Nε Coordination of Histidine to Copper

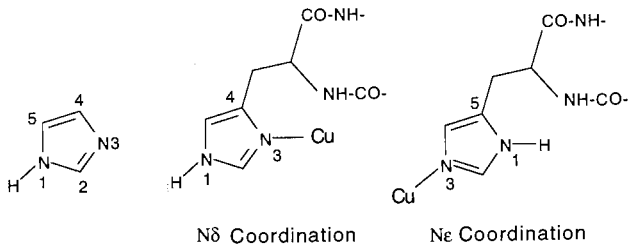

Table 6. ν_+ Frequency Associated with the Differently Substituted Imidazoles

Imidazol Type	Complex	Schematic drawing	ν_+ frequency (MHz)
Non-substituted			1.49
C4-substituted	**3**, **4**, **5**		1.49
C2-substituted	**1**, **3**		1.62
C2,C4-substituted	**3**, **4**		1.65
C2-substituted	**2**		1.30
C2,C4-substituted	**5**		1.28

Jiang et al.[1] have shown that the change in the NQI parameters can be related to the change in the occupancy of the sp^2 and pπ orbitals of the remote nitrogen of the imidazole. The model predicts that substitution on the remote nitrogen or on a carbon next to the remote nitrogen (C2 and C5; see Chart 2) perturbs the electron occupancy of these orbitals. Substitution by a methyl or an alkyl group at position C2 increases electron density around the remote nitrogen and, as a consequence, increases the electric field gradient e^2qQ. By contrast, substitution by a keto group is expected to withdraw electron density, thus to lower it on the remote nitrogen, and to yield a smaller e^2qQ. The quite significant reduction of e^2qQ observed for [Cu(BIK)$_2$](ClO$_4$)$_2$, **2**, compared to Cu(HIm)$_4$(ClO$_4$)$_2$ is attributed to the electron-withdrawing keto substitution at position C2 while alkyl substitution for [Cu(ClO$_4$)$_2$(BIM)$_2$], **1**, leads to an increase of e^2qQ. This effect is also reflected in the ν_+ frequency which can be attributed to each type of substitution of the imidazole ring as shown in Table 6. It is noteworthy that the ESEEM data for our five polyimidazole complexes also indicate that C4 substitution has a much weaker effect on the NQI parameters than C2 substitution.

Results from Cu(II) sites in biological systems have been interpreted according to the model of Jiang et al.[1] In particular, changes in the NQI parameters of the remote nitrogen of a histidine bound to Cu(II) were correlated to changes in the polarization of the N−H bond. It is noteworthy that, for a Cu(II) histidine ligand with δ coordination, the substitution is at position C4, whereas the substitution is at position C5 for ϵ coordination, i.e., at a position that is expected to have a larger influence on the NQI parameters (Chart 2). Nδ coordination has always been observed for the Cu(II) site of blue copper proteins (azurin,[41−43] cupredoxin,[44] plastocyanin,[45,46] and pseudoazurin[47]), as well as for the type I copper site of the multicopper ascorbate oxidase.[48] Moreover, it is also the case for the Cu−bleomycin complex.[49] The available NQI data for this type of copper sites and complex show that the asymmetry parameter is close to 1 and the ν_+ frequency is close to 1.5 MHz,[50−52] which are the values for $Cu(HIm)_4^{2+}$ and which are also those expected for C4-substituted imidazole ligands. By contrast, histidine ligands with Nϵ coordination have been found for the Cu(II) site of galactose oxidase[53] and for the type II copper site of ascorbate oxidase.[48] For these two enzymes, the respective e^2qQ values of 1.70 and 1.56 MHz appear larger than that observed for Nδ coordination; moreover, the asymmetry parameters appear smaller, 0.65 and 0.83 and the ν_+ frequencies are shifted to higher values 1.53 and 1.54 MHz.[1,54,50] If one assumes that substitutions at position C2 or C5, i.e., next to the remote nitrogen, will have a similar effect on the electron occupancy of the orbitals of the remote nitrogen, one expects Nϵ coordination of histidine to give the same NQI parameters as a coordinated *C2*-alkyl-substituted imidazole. Our results suggest that the ESEEM features of a Cu(II) site might reflect the Nδ or Nϵ coordination of a histidine ligand. This hypothesis must take into account the possibility of hydrogen bonding as demonstrated by Jiang et al.[1,39] and Tran et al.[40] Further work with solvents of different polarities or with *N*-methyl derivatives of the above polyimidazole ligands may clarify this point. The suggestion that the NQI parameters may be affected by whether Cu(II) binds to Nδ or Nϵ of the histidine imidazole has already been made by Goldfarb et al.[59] This question has also been addressed by Colaneri and Peisach[60,61] in their ESEEM studies of specific Cu(II) sites: Cu(II)-doped crystals of L-histidine hydrochloride monohydrate, where the Cu(II) is coordinated to the Nϵ of the imidazole ring, and of Cu(II)-doped crystals of bis(L-histidinato)cadmium dihydrate, which shows imidazole Nδ coordination of the Cu(II). Interestingly, the ESEEM parameters of the Cu(II) complex with Nϵ coordination, which reflect the properties of the remote ^{14}Nδ of the imidazole group (e^2qQ = 1.41 MHz, η = 0.66), are quite different from those of the remote ^{14}Nϵ that were measured for the Nδ-coordinated complex from the ESEEM of the other Cu(II) complex (e^2qQ = 1.57 MHz, η = 0.64). For these complexes, the contribution of the hydrogen-bonding network, in the crystal state, appears to dominate that of the inequivalence of the two remote nitrogens of the histidine imidazoles.[61] This situation differs from that of our compounds, which were studied in frozen solution, allowing the observation of a variation of the NQI parameters essentially reflecting the Nδ vs Nϵ coordination.

In addition, the spectra shown in the present study with polyimidazole ligands demonstrate that magnetically nonequivalent remote nitrogens can be distinguished by ESEEM spectroscopy, an observation already made for magnetically nonequivalent imidazoles of the Cu(II) sites of amine oxidase[55] and superoxide dismutase.[56] ESEEM data of Cu(II) complexes with substituted imidazoles may also be of interest for a comparison with those of Cu(II) sites with modified histidine ligands. A modified histidine has been found in tyrosinase where a thioether links the C2 position of the imidazole to a cysteine.[57] However, tyrosinase is a type III Cu(II) site and is not EPR detectable. Nevertheless, unusual ESEEM features of histidine remote nitrogens might help to identify modified histidine residues in copper proteins.

Conclusion

A series of new copper complexes was reported using original di-, tri-, and tetraimidazole ligands designed to mimic multihistidine sites in proteins. Various X-ray diffraction structures were obtained, with tetragonal ($[Cu(ClO_4)_2(BIM)_2]$, **1**), distorted square pyramidal ($[Cu(ClO_4)(TIM)](ClO_4)$, **4**; $[CuCl(TRIM)(CH_3OH)]Cl$, **6**), trigonal bipyramidal ($[CuCl(TIK)](ClO_4)$, **7**) and distorted tetrahedral geometries ($[Cu(BIK)_2](ClO_4)_2$, **2**) resulting from the constraints imposed by the multidentate ligands and from the properties of the counterions Cl^- and ClO_4^-. These geometries lead to a 500 mV range for the redox potentials of the various complexes from −215.5 for **4** to 248.5 mV for **2** (vs NHE). A comparative study of the complexes by ESEEM spectroscopy showed that substitution of the imidazole ring (by a methylene or a keto group) leads to a large change of the NQI parameters for C2 substitution and has no effect for C4 substitution. The electron-donating or electron-withdrawing character of the substituent leads to opposite effects on the e^2qQ parameters and on the position of the ν_+ frequency. We propose that these characteristic NQI parameters could be used to discriminate between Nδ and Nϵ coordination of histidine in copper proteins and could also reveal modified histidine ligands.

Acknowledgment. C.P. was supported by a grant from the Ministère de la Recherche et de la Technologie. We thank M. Connier and B. Champion for technical assistance.

Supporting Information Available: Tables of fractional atomic coordinates and *U* values of non-hydrogen atoms and of hydrogen atoms, anisotropic thermal parameters, interatomic bond lengths and angles, and experimental data for the crystallographic analyses (25 pages). Ordering information is given on any current masthead page.

IC9715660

(59) Goldfarb, D.; Fauth, J.-M.; Farver, O.; Pecht, I. *Appl. Magn. Reson.* **1992**, *3*, 333.
(60) Colaneri, M. J.; Peisach, J. *J. Am. Chem. Soc.* **1992**, *114*, 5335.
(61) Colaneri, M. J.; Peisach, J. *J. Am. Chem. Soc.* **1995**, *117*, 6308.